Available online at www.sciencedirect.com
ScienceDirect
Journal of Sound and Vibration 322 (2009) 954–968
JOURNAL OF SOUND AND VIBRATION
www.elsevier.com/locate/jsvi

A Bouc–Wen model compatible with plasticity postulates

A.E. Charalampakis, V.K. Koumousis*

National Technical University of Athens, Athens, Greece

Received 20 April 2008; received in revised form 7 November 2008; accepted 12 November 2008
Handling Editor: C.L. Morfey
Available online 8 January 2009

Abstract

The versatile Bouc–Wen model has been used extensively to describe hysteretic phenomena in various fields of engineering. Nevertheless, it is known that it exhibits displacement drift, force relaxation and nonclosure of hysteretic loops when subjected to short unloading–reloading paths. Consequently, it locally violates Drucker's or Ilyushin's postulate of plasticity. In this study, an effective modification of the model is proposed which eliminates these problems. A stiffening factor is introduced into the hysteretic differential equation which enables the distinction between virgin loading and reloading. Appropriate reversal points are utilized effectively to guide the entire process. It is shown that the proposed modification corrects the nonphysical behavior of the model under short unloading–reloading paths without affecting its response in all other cases. It is further demonstrated that the original and modified model exhibit significantly different response under seismic excitation.

1. Introduction

The Bouc–Wen model is a smooth phenomenological model that is often used to describe hysteretic phenomena. It was introduced by Bouc [1] and further extended by Wen [2], who investigated the random vibration of hysteretic systems. Although developed independently, it belongs to the class of endochronic models, first introduced by Valanis [3], which use the notion of intrinsic time to describe the inelastic behavior of materials.

The Bouc–Wen model has been employed successfully in many areas of engineering. Nevertheless, it is known that it suffers from displacement drift, force relaxation and nonclosure of hysteretic loops when subjected to short unloading–reloading paths. As a result, it locally violates Drucker's [4] or Ilyushin's [5] postulate of plasticity. Drucker's postulate states that the work done by an external added stress over a closed stress loop is nonnegative, while Ilyushin's postulate states that the total work done over a closed strain loop is nonnegative. These postulates are of paramount importance in classical elastoplasticity as they imply the normality rule for the plastic strain rate and the convexity of the yield surface in stress space. Ilyushin's postulate is less restrictive and characterizes the behavior of a very large class of materials, while resulting in the same consequences as Drucker's [6].

*Corresponding author. Tel.: +30 210 772 1657; fax: +30 210 772 1651.
E-mail address: vkoum@central.ntua.gr (V.K. Koumousis).

0022-460X/$ - see front matter © 2008 Elsevier Ltd. All rights reserved.
doi:10.1016/j.jsv.2008.11.017

The aforementioned deficiencies of the Bouc–Wen model have been reported repeatedly in the literature, e.g., [7–11]. To cope with this issue, a modification of the Bouc–Wen model was proposed by Casciati [8]. It involves the introduction of an additional "counterclockwise" hysteretic term which becomes effective when loading and gives rise to "negative" inelastic displacements. This modification achieves the reduction, yet not the elimination of the problem [10–12]. Notably, these violations can also be reduced by using a large value of the exponential parameter of the model. However, this approach results in an almost bilinear behavior and offers no advantage in comparison to the simple bilinear model. In addition, it reduces the accuracy achieved by using stochastic equivalent linearization techniques [13].

In this study, a simple modification is proposed which eliminates the aforementioned nonphysical behavior of the Bouc–Wen model. Thus, the long-established conclusion that "when endochronic models are adopted, local violations of the Drucker's stability postulate cannot be avoided" (Casciati and Iwan [12]) is reconsidered. The modification focuses at the root of the problem, i.e., the reduced reloading stiffness, by inserting a stiffening factor into the hysteretic differential equation. The modified model incorporates the observation that reloading after partial unloading should follow the unloading path up to the reversal point. Similar remedy was proposed by Riddell and Newmark [14] to correct the nonphysical behavior of the model by Clough and Johnston [15]. It is shown that the proposed modification eliminates the unrealistic behavior of the Bouc–Wen model with respect to short unloading–reloading paths while leaving its behavior in full hysteretic loops practically unaffected. It is further shown that, when compared to the original, the modified model may exhibit significantly different response under seismic excitation.

2. Original model formulation

The restoring force $F(t)$ of a single-degree-of-freedom system can be expressed as:

$$F(t) = a\frac{F_y}{u_y}u(t) + (1-a)F_y z(t), \tag{1}$$

where $u(t)$ is the displacement, F_y the yield force, u_y the yield displacement, a the ratio of post-yield to pre-yield (elastic) stiffness and $z(t)$ a dimensionless hysteretic parameter that obeys a single non-linear differential equation with zero initial condition:

$$\dot{z}(t) = \frac{1}{u_y}[A - |z(t)|^n(\beta + \mathrm{sgn}(\dot{u}(t)z(t))\gamma)]\dot{u}(t), \tag{2}$$

where A, β, γ, n are dimensionless quantities controlling the behavior of the model, sgn(·) is the signum function and the overdot denotes the derivative with respect to time.

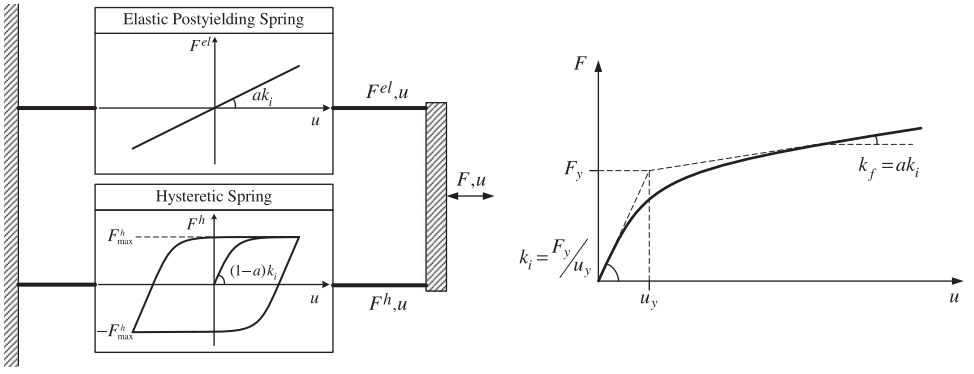

Fig. 1. Bouc–Wen model.

It follows from Eq. (1) that the restoring force $F(t)$ can be analyzed into an elastic and a hysteretic part as follows:

$$F^{el}(t) = a\frac{F_y}{u_y}u(t) \tag{3}$$

$$F^{h}(t) = (1-a)F_y z(t) \tag{4}$$

Thus, the model can be visualized as two springs connected in parallel (Fig. 1) where $k_i = F_y/u_y$ and $k_f = ak_i$ are the initial and post-yielding stiffness of the system.

3. Parameter constraints

The parameters of Bouc–Wen model are functionally redundant; there exists a multiplicity of parameter vectors that produce an identical response for a given excitation [16]. Removing this redundancy is best achieved by fixing parameter A to unity [16]. Henceforth, this constraint is assumed to hold.

4. Response

Recently, analytical expressions for the hysteretic response and dissipated energy of Bouc–Wen model were derived by the authors [17]. These expressions can be employed for the quantification of the displacement drift, the force relaxation and the violation of Ilyushin's postulate, as demonstrated in the next section. Further, they form the basis of the proposed modification as they provide the full unloading path in analytical form. For sake of completeness, these expressions are reproduced here in brief.

The behavior of Bouc–Wen model can be distinguished into four cases depending on the sign of $\dot{u}$ and z. In illustration, the response under cyclic excitation is shown in Fig. 2, where the dotted line signifies the path of the elastic response. Points A and C signify sign reversal of velocity $\dot{u}$ whereas points B and D signify sign reversal of hysteretic force F^h or, equivalently, of hysteretic parameter z.

It was shown that the displacement u is associated with the hysteretic parameter z in terms of Gauss' hypergeometric function ${}_2F_1(a,b,c;w)$ [17]. In the non-trivial case of $\beta \neq \gamma$, the following relation holds:

$$\frac{u-u_0}{u_y} = z\,{}_2F_1\left(1, \frac{1}{n}, 1+\frac{1}{n}; q|z|^n\right)\Bigg|_{z_0}^{z}, \tag{5}$$

where $q = \beta + \mathrm{sgn}(\dot{u}z)\gamma$ and u_0, z_0 are the initial values of the displacement and hysteretic parameter, respectively. Eq. (5) can be used with arbitrary values of n, β and γ provided that q does not change during the transition under consideration. Proper evaluation techniques for the hypergeometric function are provided in Appendix A while simpler relations will be produced for specific values of the exponential parameter. Thus, for $n = 1$ Eq. (5) is solved analytically for z as follows [17]:

$$z = \frac{\mathrm{sgn}(z) + (qz_0 - \mathrm{sgn}(z))\mathrm{e}^{-\mathrm{sgn}(z)q(u-u_0)/u_y}}{q} \tag{6}$$

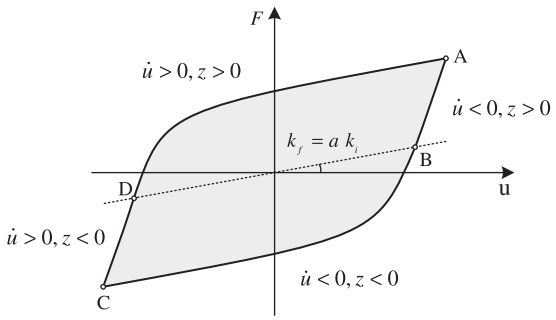

Fig. 2. Response of Bouc–Wen model under cyclic excitation.

Table 1
Values of q and sgn(z) per segment.

Segment	q	sgn(z)
AB	$\beta-\gamma$	$+1$
BC	$\beta+\gamma$	-1
CD	$\beta-\gamma$	-1
DA	$\beta+\gamma$	$+1$

For $n=2$, z is given by Ref. [17]:

$$z=\frac{\tanh(\sqrt{q}(u-u_0)/u_y+\operatorname{arctanh}(\sqrt{q}z_0))}{\sqrt{q}}, \tag{7}$$

where $\tanh(\cdot)$, $\operatorname{arctanh}(\cdot)$ are the normal and inverse hyperbolic tangent, respectively. In Eq. (7), $\sqrt{q}$ may be complex but the result is real. Special attention must be paid with respect to the values of q and sgn(z) per segment (Table 1).

In the special case of $\beta=\gamma$, the unloading branches are straight lines and integration of Eq. (2) yields:

$$z=\frac{(u-u_0)}{u_y}+z_0 \tag{8}$$

Eq. (8) is independent of n. The loading branches are covered by Eq. (5).

5. Deficiencies of original model

5.1. Displacement drift

The hysteretic spring of the model (Fig. 1) exhibits displacement drift when cycled between two unequal forces F_1^h, F_2^h with $F_{\max}^h \geqslant F_1^h > F_2^h \geqslant 0$. Referring to Fig. 3a, the displacement drift d can be quantified easily for arbitrary values of n, β and γ by employing Eq. (5) in the transition between points $A \to B \to D$. Note that $F_{\max}^h=(1-a)F_y$, $z_A=z_D=F_1^h/F_{\max}^h$, $z_B=F_2^h/F_{\max}^h$, while $F_A \neq F_D$ due to the contribution of the elastic spring. When $n=1$, the drift is expressed as:

$$d_1=u_y\left(\frac{1}{q_n}\ln\left(\frac{F_{\max}^h-q_nF_1^h}{F_{\max}^h-q_nF_2^h}\right)+\frac{1}{q_p}\ln\left(\frac{F_{\max}^h-q_pF_2^h}{F_{\max}^h-q_pF_1^h}\right)\right), \tag{9}$$

where $q_p=\beta+\gamma$, $q_n=\beta-\gamma$ and $\ln(\cdot)$ is the natural logarithm. When $n=2$, the drift is given by:

$$d_2=u_y\left(\frac{\operatorname{arctanh}\left(\frac{\sqrt{q_n}F_2^h}{F_{\max}^h}\right)-\operatorname{arctanh}\left(\frac{\sqrt{q_n}F_1^h}{F_{\max}^h}\right)}{\sqrt{q_n}}+\frac{\operatorname{arctanh}\left(\frac{\sqrt{q_p}F_1^h}{F_{\max}^h}\right)-\operatorname{arctanh}\left(\frac{\sqrt{q_p}F_2^h}{F_{\max}^h}\right)}{\sqrt{q_p}}\right) \tag{10}$$

In case $\beta=\gamma$, the unloading branch is covered by Eq. (8) and hence Eqs. (9) and (10) are modified, respectively, as follows:

$$d_1^*=u_y\left(\frac{F_2^h-F_1^h}{F_{\max}^h}+\frac{1}{q_p}\ln\left(\frac{F_{\max}^h-q_pF_2^h}{F_{\max}^h-q_pF_1^h}\right)\right) \tag{11}$$

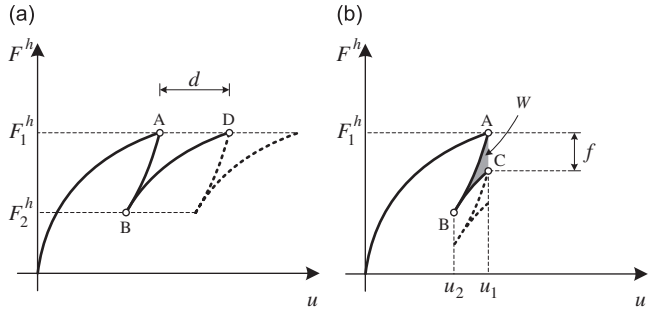

Fig. 3. (a) Displacement drift and (b) force relaxation of hysteretic spring.

$$d_2^* = u_y \left(\frac{F_2^h - F_1^h}{F_{\max}^h} + \frac{\operatorname{arctanh}\left(\frac{\sqrt{q_p} F_1^h}{F_{\max}^h}\right) - \operatorname{arctanh}\left(\frac{\sqrt{q_p} F_2^h}{F_{\max}^h}\right)}{\sqrt{q_p}} \right) \tag{12}$$

5.2. Force relaxation

The hysteretic spring exhibits force relaxation when cycled between two unequal displacements u_1, u_2 with $u_1 > u_2$. Referring to Fig. 3b, the force relaxation f can be quantified by utilizing Eqs. (6) and (7) over the transition $A \to B \to C$ in which the hysteretic force does not change sign. When $n = 1$, it is given by:

$$f_1 = \frac{(e_p - e_n) F_1^h}{e_p} + \frac{F_{\max}^h (e_n - 1)}{e_p q_n} + \frac{F_{\max}^h (1 - e_p)}{e_p q_p}, \tag{13}$$

where $e_p = \exp(q_p \Delta u / u_y)$, $e_n = \exp(q_n \Delta u / u_y)$ and $\Delta u = u_1 - u_2$. For $n = 2$, the force relaxation is expressed as:

$$f_2 = F_1^h - \frac{F_{\max}^h}{\sqrt{q_p}} \tanh\left(\frac{\sqrt{q_p} \Delta u}{u_y} - \operatorname{arctanh}\left(\frac{q_p \tanh\left(\frac{\sqrt{q_n} \Delta u}{u_y} - \operatorname{arctanh}\left(\frac{\sqrt{q_n} F_1^h}{F_{\max}^h} \right) \right)}{\sqrt{q_p q_n}} \right) \right) \tag{14}$$

In case $\beta = \gamma$ the unloading branch is covered by Eq. (8) and hence Eqs. (13) and (14) are modified, respectively, as follows:

$$f_1^* = \frac{\Delta u F_{\max}^h}{e_p u_y} + \frac{(e_p - 1)(q_p F_1^h - F_{\max}^h)}{q_p e_p} \tag{15}$$

$$f_2^* = F_1^h - \frac{F_{\max}^h}{\sqrt{q_p}} \tanh\left(\frac{\sqrt{q_p} \Delta u}{u_y} + \operatorname{arctanh}\left(\sqrt{q_p} \left(\frac{F_1^h}{F_{\max}^h} - \frac{\Delta u}{u_y} \right) \right) \right) \tag{16}$$

5.3. Ilyushin's postulate

Regarding the Bouc–Wen model, the work of the elastic spring over a closed strain loop is zero. Thus, in violation of Ilyushin's postulate, the total work W over the transition $A \to B \to C$ of Fig. 3b is attributed to the hysteretic spring only and it is expressed by the shaded area with a negative sign. It is noted that W is *not* equal to the dissipated energy [18]. If it were, the model would violate the second law of thermodynamics [19].

The total work W over the transition $A \to B \to C$ in which the hysteretic force does not change sign is given by:

$$W = F^h_{\max} u_y \left(\int_{z_A}^{z_B} \frac{z}{1-(\beta-\gamma)z^n}\,\mathrm{d}z + \int_{z_B}^{z_C} \frac{z}{1-(\beta+\gamma)z^n}\,\mathrm{d}z \right) \tag{17}$$

When $n = 1$, the total work is expressed as:

$$W_1 = F^h_{\max} u_y \left(\frac{q_n(z_A - z_B) + \ln\left(\dfrac{1-q_n z_A}{1-q_n z_B}\right)}{q_n^2} + \frac{q_p(z_B - z_C) + \ln\left(\dfrac{1-q_p z_B}{1-q_p z_C}\right)}{q_p^2} \right), \tag{18}$$

where $z_A = F^h_1/F^h_{\max}$ and z_B, z_C are determined by successive application of Eq. (6). For $n = 2$, the total work is given by:

$$W_2 = \frac{F^h_{\max} u_y}{2} \left(\frac{1}{q_n} \ln\left(\frac{1-q_n z_A^2}{1-q_n z_B^2}\right) + \frac{1}{q_p} \ln\left(\frac{1-q_p z_B^2}{1-q_p z_C^2}\right) \right), \tag{19}$$

where z_B, z_C are determined by successive application of Eq. (7).

In case $\beta = \gamma$, the unloading branch is covered by Eq. (8) and hence Eqs. (18) and (19) are modified, respectively, as follows:

$$W_1^* = F^h_{\max} u_y \left(\frac{z_B^2 - z_A^2}{2} + \frac{q_p(z_B - z_C) + \ln\left(\dfrac{1-q_p z_B}{1-q_p z_C}\right)}{q_p^2} \right) \tag{20}$$

$$W_2^* = \frac{F^h_{\max} u_y}{2} \left(z_B^2 - z_A^2 + \frac{1}{q_p} \ln\left(\frac{1-q_p z_B^2}{1-q_p z_C^2}\right) \right) \tag{21}$$

6. Modified model

In this section, an efficient modification is proposed for the correction of the nonphysical behavior of Bouc–Wen model. The modification is built progressively and the reasoning behind each step is discussed.

The root of the problem is that the model predicts reduced loading stiffness as compared to the unloading one at the same point. Thus, a mechanism for controlling the stiffness between these two extreme values is needed. To this purpose, Eq. (2) is modified as follows:

$$\dot{z} = \frac{1}{u_y}[A - |z|^n(\beta + (\mathrm{sgn}(\dot{u}z)\,\underline{-2H(\dot{u}z)R_s(u,z)})\gamma)]\dot{u}, \tag{22}$$

where the underlined expression is the modification, $R_s(u,z) \in [0,1]$ is a stiffening factor and $H(\cdot)$ is the Heaviside function defined herein as:

$$H(x) = \begin{cases} 1, x > 0 \\ 0, x \leqslant 0 \end{cases}. \tag{23}$$

Note that definition (23) differs from the one in [20] at $x = 0$. Due to the Heaviside function, the unloading branches of the modified model remain identical to those of the original model. When loading or reloading, factor $R_s(u,z)$ controls the transition between loading (reduced) stiffness and unloading (increased) stiffness. For $R_s = 0$, Eq. (22) reduces to Eq. (2) and the proposed modified model is identical to the original one. For $R_s = 1$, the loading stiffness becomes equal to that of unloading at the same point.

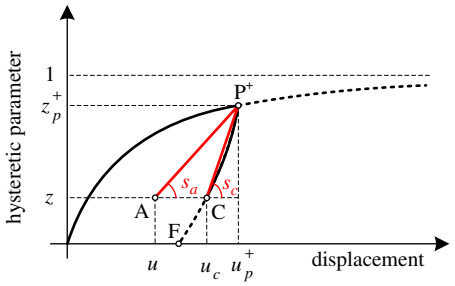

Fig. 4. Formulation of stiffening factor R_s.

Next, a consistent formulation of stiffening factor R_s is considered. By virtue of Eqs. (5) and (8), the full unloading path from a reversal point is known *a priori* in analytical form. For $\beta \neq \gamma$ this path is curved, whereas for $\beta = \gamma$ it is a straight line. Setting R_s equal to unity along this path has the desired effect that partial unloading followed by reloading will guide the hysteretic response exactly on the unloading path up to the reversal point. Upon there, factor R_s should revert to zero to allow for further loading with normal (reduced) stiffness. Finally, factor R_s should diminish in regions away from the unloading path so that normal behavior of Bouc–Wen model remains unaffected.

Based on these observations, a suitable expression of $R_s(u,z)$ is defined. In illustration, we assume that $P^+(u_p^+, z_p^+)$ is a reversal point in the upper half-plane of the u–z space ($z_p^+ > 0$). Symmetric formulation with respect to the origin of the reference axes is assumed for the lower half-plane. During reloading, it is assumed that the current state is represented by point $A(u,z)$ with $0 \leqslant z < z_p^+$ (Fig. 4). Point $C(u_c, z)$ is the corresponding point of the unloading path. By employing Eqs. (5) and (8), u_c is given by Eqs. (24) and (25) for $\gamma \neq \beta$ and $\gamma = \beta$, respectively, as:

$$u_c(z) = u_y z_2 F_1\left(1, \frac{1}{n}, 1+\frac{1}{n}; (\beta-\gamma)z^n\right)\Big|_{z_p^+}^{z} + u_p^+ \tag{24}$$

$$u_c^*(z) = (z - z_p^+)u_y + u_p^+ \tag{25}$$

A natural way of controlling stiffness in the u–z space is based on the slopes in the same space. We denote s_a the slope of line AP^+, as opposed to the "critical" slope s_c of line CP^+. Referring to Fig. 4, it follows that $s_a/s_c = (u_p^+ - u_c(z))/(u_p^+ - u)$. Based on this ratio, a simple expression for the factor R_s is proposed as:

$$R_s(u,z) = H(z_p^+ - z)H(u_c(z) - u)\left(\frac{u_p^+ - u_c(z)}{u_p^+ - u}\right)^p, \tag{26}$$

where $p \geqslant 1$ is a constant. As point A approaches point C from the left, factor R_s increases and approaches unity. When points A and C coincide, $R_s = 1$ and loading follows the unloading path exactly. Thus, the unloading path $P^+ - F$ is a "horizon", i.e., it cannot be crossed. When z is greater than z_p^+ or u is greater than u_c, the stiffening effect disappears due to the Heaviside functions of Eq. (26). Parameter p controls the intensity of stiffening to the left of the unloading path. For increased values of p, stiffening is concentrated close to the unloading path and diminished everywhere else. In general, it was observed that values of p between 1.0 and 2.0 produce realistic hysteretic behavior.

To demonstrate the effect of the proposed modification, we consider a system with $n = 2$, $\beta = 0.1$, $\gamma = 0.9$ which is subjected to virgin loading. Unloading occurs when $u_p^+ = 1.5u_y$ and $z_p^+ \cong 0.905$. We impose a displacement to the negative direction and then back to the positive direction. Applying the stiffening rule with $p = 2$ has a profound effect on the response of the hysteretic spring. In illustration, Fig. 5 shows cases (a)–(d) where loading in the negative direction reaches u_y, $0.5u_y$, 0 and $-1.5u_y$, respectively. It is demonstrated that the differences in the response depend on the intensity of the reversal. In cases (a,b and c), the nonphysical behavior of Bouc–Wen model is corrected, whereas in case (d) the response of the original and modified model are practically identical. In case a1, application of Eqs. (10), (14) and (19) yield displacement

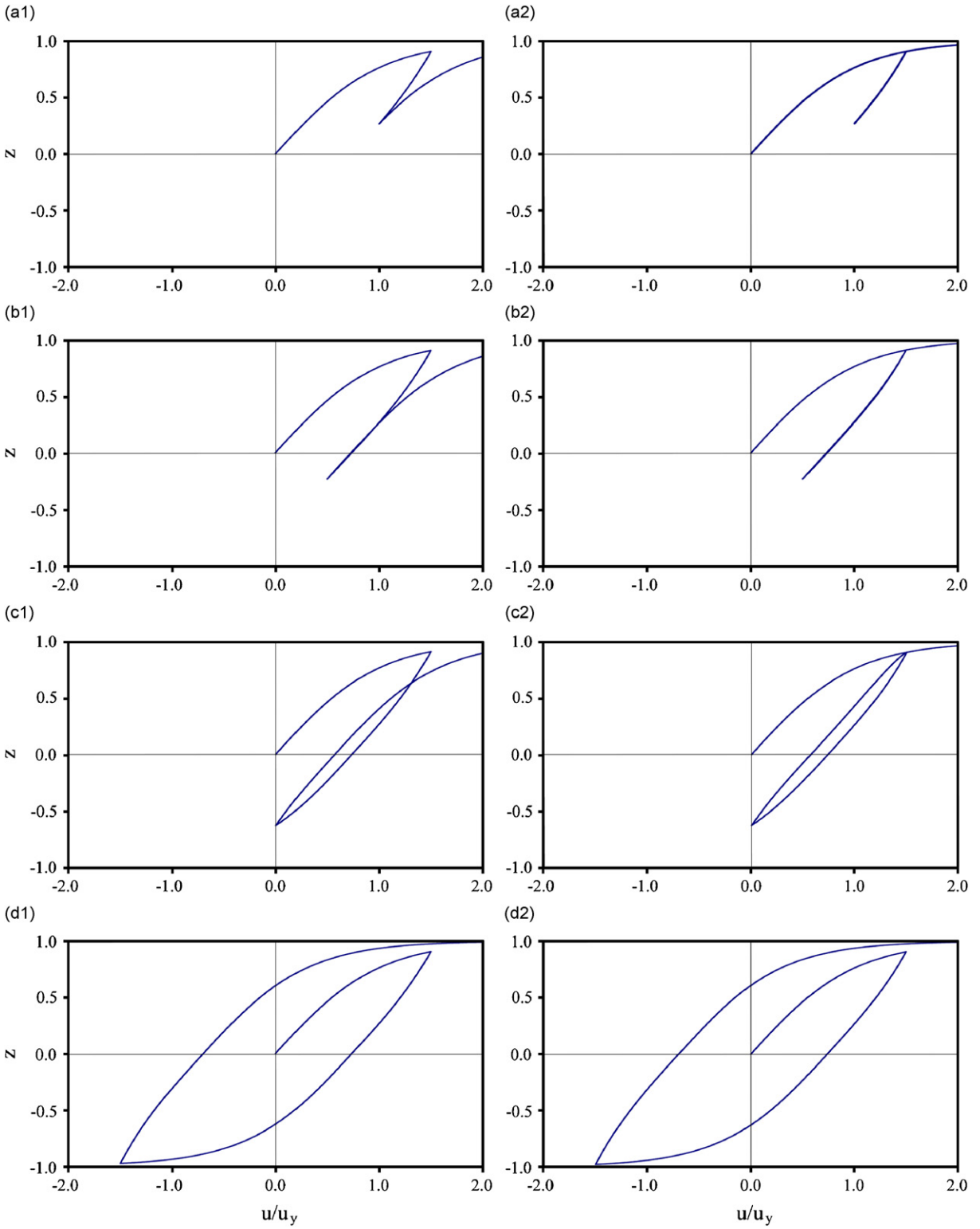

Fig. 5. Stiffening effect in u–z space: original model (left), modified model (right) ($n = 2$, $\beta = 0.1$, $\gamma = 0.9$, $u_p^+ = 1.5u_y$, $z_p^+ \approx 0.905$, $p = 2$).

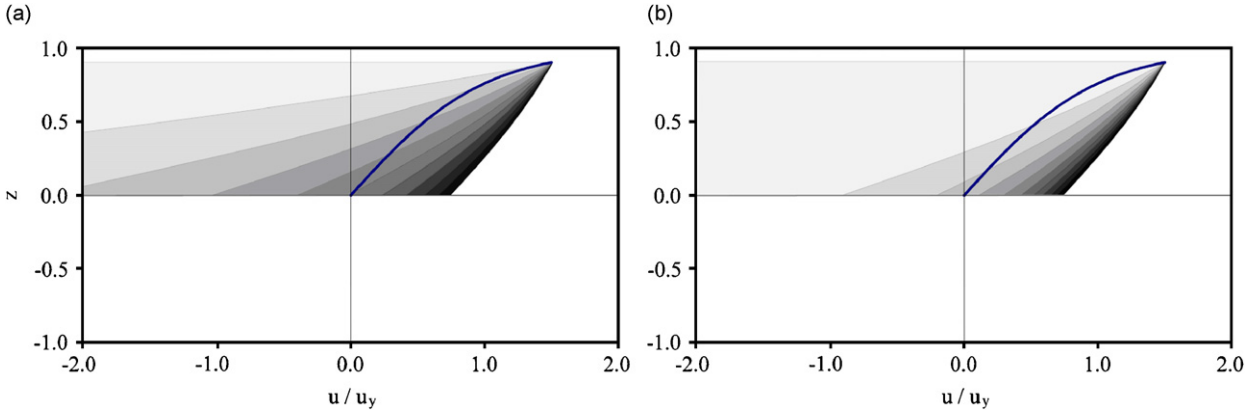

Fig. 6. Contour plot of R_s with $n = 2$, $\beta = 0.1$, $\gamma = 0.9$, $u_p^+ = 1.5u_y$, $z_p^+ \approx 0.905$ and (a) $p = 1.0$, (b) $p = 2.0$.

drift of $d \cong 0.728u_y$, force relaxation of $f \cong 0.257F^h_{\max}$ and violation of Ilyushin's postulate of $W \cong -0.044756F^h_{\max}u_y$, respectively.

In addition, Fig. 6 shows the contour plots of stiffening factor R_s in case of $p = 1$ and $p = 2$. These plots are fully defined upon establishment of reversal point $P^+(1.5u_y, 0.905)$. The darker a point is, the more intense is the stiffening effect at that point during reloading. The edge of the darkest area is the unloading path, along which $R_s = 1$ irrespectively of p. It is shown that for $p = 2$ stiffening is concentrated close to the unloading path.

7. Selection of reversal point

The effectiveness of the proposed modification was demonstrated for the case of a single reversal point. Nevertheless, for a system under random excitation a critical issue arises regarding *which* reversal point should be used. In order to facilitate algorithmic implementation, the following investigation is based on discrete time instants t_i with $i = 0, 1, 2, \ldots$ and $t_0 = 0$. All expressions refer to the upper half-plane of the u–z space; symmetric formulation with respect to the origin of the reference axes is assumed for the lower half-plane.

As first attempt, we may employ the last observed reversal point. The set of time instants that correspond to reversals up to time t_i (with $i \geqslant 2$) can be written as:

$$T_i^+ = \{t_j | u(t_{j-1}) < u(t_j) \wedge u(t_j) > u(t_{j+1}) \wedge z(t_j) > 0,\ j = \{1, 2, \ldots, i-1\}\} \tag{27}$$

Therefore, the set T_i^+ contains all time instants upto t_i for which the displacement exhibits local maxima and the hysteretic parameter is positive. The time instant of the last observed reversal point is given simply as:

$$t_i^+ = \max T_i^+ \tag{28}$$

However, this formulation may cancel the desired stiffening effect when multiple reversals of small amplitude are involved. In illustration, we consider a system with the following properties: $\beta = 0.1$, $\gamma = 0.9$, $a = 0.10$, $n = 2.0$, $F_y = 2.86\,\text{kN}$, $u_y = 0.111\,\text{m}$, $m = 13\,\text{kNs}^2/\text{m}$ and $p = 2.0$. For the following analyses, the Northridge TAR090 excitation is used [21]. The aforementioned undesired behavior is manifested in details A and B of Fig. 7.

A different approach involves the reversal point that maximizes displacement. The set of these time instants is given as:

$$\bar{T}_i^+ = \{t_j \in T_i^+ | u(t_j) \geqslant u(t_k),\ \forall t_k \in T_i^+\} \subseteq T_i^+ \tag{29}$$

If $\bar{T}_i^+$ contains more than one element, the last time instant that maximizes z is selected:

$$t_i^+ = \max\{t_j \in \bar{T}_i^+ | z(t_j) \geqslant z(t_k),\ \forall t_k \in \bar{T}_i^+\} \tag{30}$$

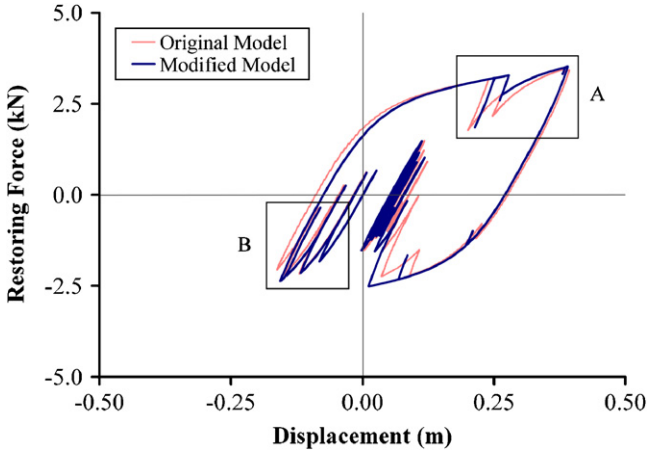

Fig. 7. Response under the Northridge TAR090 [21] excitation using last observed reversal points.

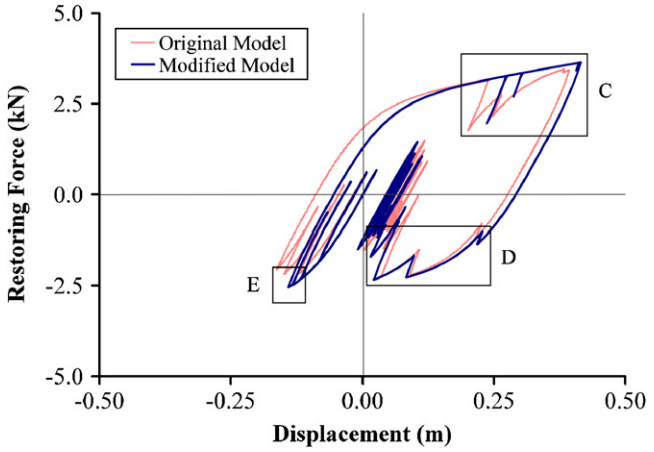

Fig. 8. Response under the Northridge TAR090 [21] excitation using maximum displacement reversal points.

This formulation may not be effective for all cases, as shown in Fig. 8. Although the model behaves as expected when loading in the positive direction (Detail C), it is shown that the stiffening effect in detail D is inadequate because the current minimum displacement reversal point lies in detail E.

In order to cover all cases, one has to take into account multiple reversal points. Therefore, it is important to investigate the conditions under which a reversal point should be considered "active".

When a reversal point $P^+(u_p^+, z_p^+)$ is established, a symmetric zone is defined in u–z space where $z \in (-z_p^+, z_p^+)$. Within this zone, P^+ is "active" in the sense that any single unloading–reloading path of the original Bouc–Wen model falls below P^+ (Fig. 9). At the limit, a path for which the hysteretic parameter varies in the sequence $z_p^+ \to -z_p^+ \to z_p^+$ will be guided to P^+ exactly. The proof is provided in Appendix B. Based on these observations, stiffening is required for excursions within this zone, so that the path of the hysteretic response will be guided either through or over P^+. If z somehow falls outside this zone, P^+ is not considered active for the remaining process. Based on this formulation, the set of "active" reversal points at time t_i is defined as:

$$\tilde{T}_i^+ = \{t_j \in T_i^+ | z(t_k) \in (-z(t_j), z(t_j)),\ \forall t_k \in \{t_{j+1}, t_{j+2}, \ldots, t_i\}\} \subseteq T_i^+ \tag{31}$$

which contains the time instants that correspond to reversals for which the hysteretic parameter remains within their respective "active" zone up to t_i. At each time instant t_i, the stiffening factors that correspond to

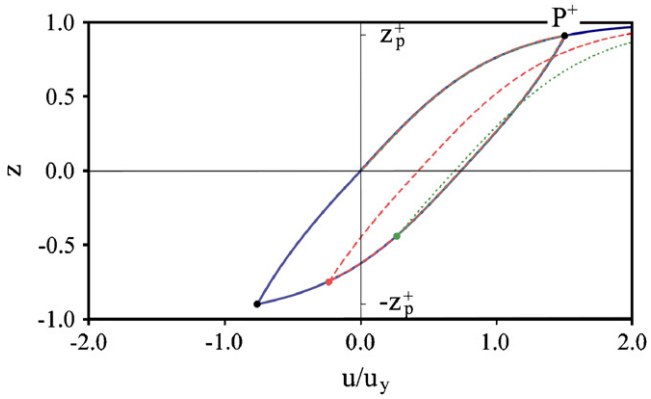

Fig. 9. "Active" zone of reversal point P^+ ($n=2$, $\beta=0.1$, $\gamma=0.9$, $u_p^+=1.5u_y$, $z_p^+\approx 0.905$).

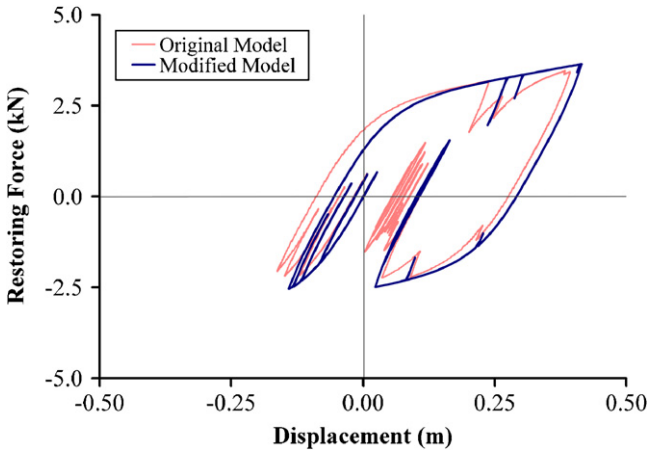

Fig. 10. Response under the Northridge TAR090 [21] excitation using multiple reversal points.

all $t_i^+ \in \tilde{T}_i^+$ are evaluated and the maximum one is used. When employing this definition in the previous example, it is observed that all intermediate reversals are correctly ignored (Fig. 10). These include the reversals at the end of the event, which cause considerable drift in the original model.

Therefore, by using relations (22), (26) and (31) one can correct all aforementioned deficiencies which were attributed to the Bouc–Wen model in the past.

Programming of the proposed modification is straightforward and is implemented at each integration step by (a) adding the stiffening term into the differential equation, (b) evaluating and employing the maximum stiffening factor R_s that corresponds to "active" reversal points using relation (26) and (c) updating the set of "active" reversal points. The latter is accomplished effectively by adding into the set the new reversal points and removing existing ones that have become "inactive".

8. Comparison of original and modified model

Based on the previous results, it is evident that the overall response of the modified model may be considerably different from that of the original. The differences depend on the number and extent of short reversals, especially those that occur when the hysteretic spring has yielded in either direction. Referring to Fig. 10, this observation is clear when loading in the positive direction.

In addition, for design purposes we are interested in the peak values of certain time histories. We measure the relative error of the peak values as follows:

$$\varepsilon = \frac{\max(\bar{y}(t)) - \max(y(t))}{\max(y(t))}, \tag{32}$$

where $y(t)$ and $\bar{y}(t)$ are the time histories corresponding to the original and modified model, respectively, and $\max(\cdot)$ denotes the maximum absolute value.

We consider a specific system with the following properties: $\beta = 0.1$, $\gamma = 0.9$, $a = 0.10$, $n = 2.0$, $F_y = 2.86\,\text{kN}$, $u_y = 0.111\,\text{m}$. Regarding the modified model, the formulation with multiple reversal points is employed with $p = 2.0$. The plastic period is controlled by changing the mass of the system. For a selection of 20 strong motion recordings [21] (Table 2), Figs. 11 and 12 show the envelope of the relative error in the peak displacement and peak hysteretic energy, respectively. The results have been filtered to include cases for which

Table 2
Strong motion recordings taken from PEER [21].

#	Title	PGA (g)	PGV (cm/s)	PGD (cm)
1	ChiChi CHY028 N	0.821	67.0	23.28
2	ChiChi CHY028 W	0.653	72.8	14.68
3	ChiChi TCU084 N	0.417	45.6	21.27
4	ChiChi TCU084 W	1.157	114.7	31.43
5	Kobe Takatori TAK000	0.611	127.1	35.77
6	Kobe Takatori TAK090	0.616	120.7	32.72
7	Northridge Rinaldi RRS228	0.838	166.1	28.78
8	Northridge Rinaldi RRS318	0.472	73.0	19.76
9	Northridge Tarzana TAR090	1.779	113.6	33.22
10	Northridge Tarzana TAR360	0.990	77.6	30.45
11	Kocaeli Duzce DZC180	0.312	58.8	44.11
12	Kocaeli Duzce DZC270	0.358	46.4	17.61
13	Tabas TAB-LN	0.836	97.8	36.92
14	Tabas TAB-TR	0.852	121.4	94.58
15	Imperial Valley I-ELC180	0.313	29.8	13.32
16	Imperial Valley I-ELC270	0.215	30.2	23.91
17	Loma Prieta GPC000	0.563	94.8	41.18
18	Loma Prieta GPC090	0.605	51.0	11.50
19	Erzikan ERZ-NS	0.515	83.9	27.35
20	Erzikan ERZ-EW	0.496	64.3	22.78

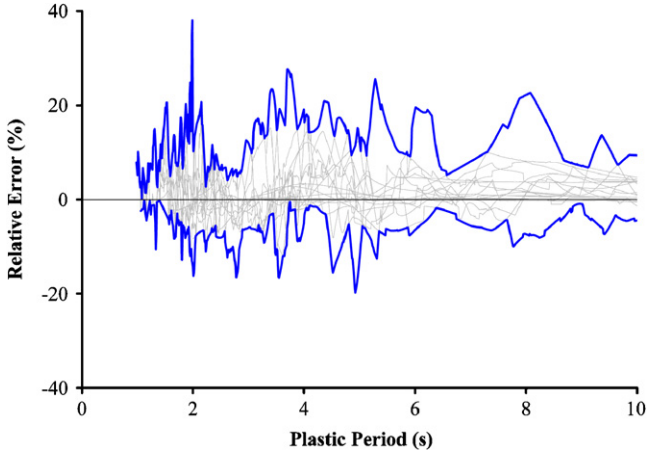

Fig. 11. Relative peak displacement error.

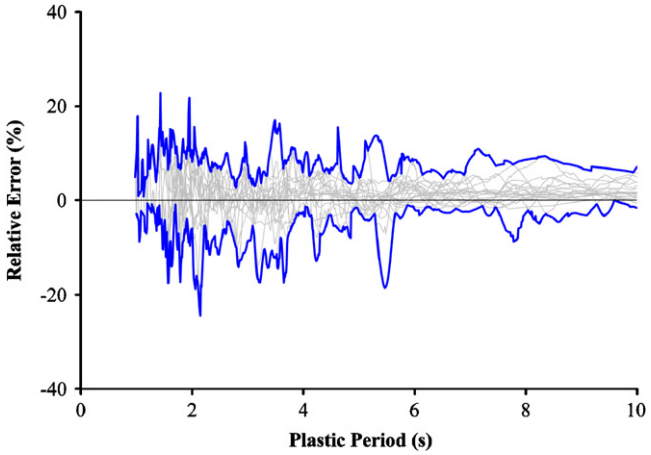

Fig. 12. Relative peak hysteretic energy error.

$\max(u(t)) \geqslant u_y$ or $\max(\bar{u}(t)) \geqslant u_y$. Thus, only the results that involve an appreciable level of hysteretic damping are displayed. It is observed that the peak values of the modified model may be smaller or larger than that of the original one. For the excitations considered herein, the relative error may reach 38% and 24% for the peak displacement and peak hysteretic energy, respectively.

It is noted that the difference in the overall response may or may not be reflected to the peak values. For example, it frequently results that the difference in the peak displacement between the original and modified model is exactly zero, as this occurs during virgin loading i.e., in the absence of any stiffening effect.

9. Conclusions

A simple modification of the versatile Bouc–Wen model is proposed which results in the correction of its nonphysical behavior when subjected to short unloading–reloading paths. This behavior is manifested as displacement drift, force relaxation and nonclosure of hysteretic loops, which result into violation of Drucker's or Ilyushin's postulate. These phenomena are quantified based on analytical relations that were derived recently by the authors [17]. The proposed modification is based on the introduction of a suitable stiffening factor which is inserted directly into the hysteretic differential equation. This results in a distinction between virgin loading and reloading, a feature that is absent in the original model. The notion of "active" reversal points is defined which controls the entire process effectively. The proposed modifications are explained in detail and their effects are demonstrated and discussed. Finally, it is shown that the original and modified model may exhibit significantly different response under seismic excitation.

The proposed modification can be applied to extended Bouc–Wen models that also take into account degradation phenomena, e.g. [23]. This is feasible since the modification focuses in the hysteretic spring only and it is fully formulated within the u–z space.

Acknowledgments

This work has been funded by the project PENED 2003. The project is co-financed 80% of public expenditure through EC-European Social Fund, 20% of public expenditure through Ministry of Development—General Secretariat of Research and Technology and through private sector, under measure 8.3 of Operational Programme "Competitiveness" in the 3rd Community Support Programme.

Appendix A. Evaluation of Gauss' hypergeometric function

The hypergeometric function is the analytical continuation of the so-called hypergeometric series [20]:

$$ {}_2F_1(a,b,c;w)=\sum_{n=0}^{\infty}\frac{(a)_n(b)_n}{(c)_n}\frac{w^n}{n!}, \tag{33}$$

where $(w)_n=w(w+1)\dots(w+n-1),(w)_0=1$ is Pochhammer's symbol and $n!$ the factorial of n.

In this study, one is interested in the evaluation of ${}_2F_1(a,b,c;w)$ for real values of $w\in(-\infty,1)$. Although the circle of convergence of series (33) is the unit circle $|w|=1$, its rate of convergence is satisfactory only for $|w|\leqslant 1/2$ [22]. For $w\in(1/2,1)$, the values are produced by linear transformation. In the cases presented herein, $c=a+b$ and hence the following formula is used [20]:

$$ {}_2F_1(a,b,a+b;w)=\frac{\Gamma(a+b)}{\Gamma(a)\Gamma(b)}\sum_{n=0}^{\infty}\frac{(a)_n(b)_n}{(n!)^2}[2\psi(n+1)-\psi(a+n)-\psi(b+n)-\ln(1-w)](1-w)^n, \tag{34}$$

where $\Gamma(\cdot)$ is the Gamma function, $\psi(\cdot)$ the Psi (Digamma) function and $\ln(\cdot)$ the natural logarithm. In general, Eq. (34) exhibits satisfactory rate of convergence even when evaluating the limit of the hypergeometric function as $w\to 1^-$. Finally, for $w\in(-\infty,-1/2)$, the following linear transformation is used [20]:

$$ {}_2F_1(a,b,c;w)=(1-w)^{-a}\,{}_2F_1\left(a,c-b,c;\frac{w}{w-1}\right) \tag{35}$$

The new function evaluation falls into one of the cases covered by Eqs. (33) and (34).

Appendix B. Proof

Regarding Fig. 9, we will prove that, beginning at $P^+(u_p^+,z_p^+)$, a hysteretic loop for which z varies in the sequence $z_p^+\to -z_p^+\to z_p^+$ will be guided to P^+ exactly.

We assume that the final point is $\hat{P}^+(\hat{u}_p^+,z_p^+)\neq P^+$. The hysteretic loop can be analyzed into the sequence $P^+\to P_1(u_1,0)\to P_2(u_2,-z_p^+)\to P_3(u_3,0)\to \hat{P}^+$. By successive application of Eq. (5), one obtains:

$$ \frac{u_1-u_p^+}{u_y}=0-z_p^+\,{}_2F_1\left(1,\frac{1}{n},1+\frac{1}{n};(\beta-\gamma)|z_p^+|^n\right) \tag{36}$$

$$ \frac{u_2-u_1}{u_y}=-z_p^+\,{}_2F_1\left(1,\frac{1}{n},1+\frac{1}{n};(\beta+\gamma)|-z_p^+|^n\right)-0 \tag{37}$$

$$ \frac{u_3-u_2}{u_y}=0-\left[-z_p^+\,{}_2F_1\left(1,\frac{1}{n},1+\frac{1}{n};(\beta-\gamma)|-z_p^+|^n\right)\right] \tag{38}$$

$$ \frac{\hat{u}_p^+-u_3}{u_y}=z_p^+\,{}_2F_1\left(1,\frac{1}{n},1+\frac{1}{n};(\beta+\gamma)|z_p^+|^n\right)-0 \tag{39}$$

By adding Eqs. (36)–(39) by parts, one obtains $\hat{u}_p^+=u_p^+$. Thus, $\hat{P}^+=P^+$.

References

[1] R. Bouc, Forced vibration of mechanical systems with hysteresis, *Proceedings of the Fourth Conference on Non-linear Oscillation*, Prague, Czechoslovakia, 1967.
[2] Y.K. Wen, Method for Random Vibration of Hysteretic Systems, *Journal of the Engineering Mechanics Division* 102 (EM2) (1976) 249–263.
[3] K.C. Valanis, A theory of viscoplasticity without a yield surface, Part I: general theory, *Archives of Mechanics* 23 (4) (1971) 517–533.
[4] D.C. Drucker, Some implications of work hardening and ideal plasticity, *Quarterly of Applied Mathematics* 7 (1950) 411–418.
[5] A.A. Ilyushin, On the postulate of plasticity, *Prikladnaya Matematika i Mekhanika* 25 (1961) 503–507.

[6] Y.F. Dafalias, Il'iushin's postulate and resulting thermodynamic conditions on elasto-plastic coupling, *International Journal of Solids and Structures* 13 (1977) 239–251.
[7] I.S. Sandler, On the uniqueness and stability of endochronic theories of material behavior, *Journal of Applied Mechanics* 45 (1978) 263–266.
[8] F. Casciati, Non-linear stochastic dynamics of large structural system by equivalent linearization, *Proceedings ICASP5*, Vancouver, 1987, pp. 1165–1172.
[9] R.S. Thyagarajan, Modeling and analysis of hysteretic structural behavior, Report No. EERL-89-03, Earthquake Engineering Research Laboratory, California Institute of Technology, Pasadena, CA, 1989.
[10] E. Spacone, V. Ciampi, F.C. Philippou, A beam element for seismic damage analysis, Report No. UCB/EERC-92/07, Earthquake, Engineering Research Center, University of California, Berkeley, 1992.
[11] C.W. Wong, Y.Q. Ni, J.M. Ko, Steady-state oscillation of hysteretic differential model II: performance analysis, *Journal of Engineering Mechanics* 120 (11) (1994) 2299–2325.
[12] F. Casciati, Stochastic dynamics of hysteretic media, *Structural Safety* 6 (1989) 259–269.
[13] F. Casciati, L. Faravelli, M.P. Singh, Non-linear structural response and modeling uncertainty on system parameters and seismic excitation, *Proceedings Eighth ECEE*, Lisbon, 1986, 6.3, pp. 41–48.
[14] R. Riddell, N.M. Newmark, Force-deformation models for non-linear analysis, *Journal of Structural Division* 105 (ST12) (1979) 2773–2778.
[15] R.W. Clough, S.B. Johnston, Effect of stiffness degradation on earthquake ductility requirements, *Proceedings of the Japan Earthquake Engineering Symposium*, Tokyo, Japan, 1966.
[16] F. Ma, H. Zhang, A. Bockstedte, G.C. Foliente, P. Paevere, Parameter analysis of the differential model of hysteresis, *Journal of Applied Mechanics ASME* 71 (2004) 342–349.
[17] A.E. Charalampakis, V.K. Koumousis, On the response and dissipated energy of Bouc–Wen hysteretic model, *Journal of Sound and Vibration* 309 (2008) 887–895.
[18] K.C. Valanis, On the substance of Rivlin's remarks on the endochronic theory, *International Journal of Solids and Structures* 17 (1981) 249–265.
[19] M. Sasani, E.P. Popov, Seismic energy dissipators for RC panels: analytical studies, *ASCE Journal of Engineering Mechanics* 127 (8) (2001) 835–843.
[20] M. Abramowitz, I.A. Stegun, *Handbook of Mathematical Functions*, National Bureau of Standards, Washington, Dover Publications, New York (reprinted on 1972).
[21] Pacific Earthquake Engineering Research Centre (PEER), Strong ground motion database 2006 ⟨http://peer.berkeley.edu/⟩.
[22] W.H. Press, S.A. Teukolsky, W.T. Vetterling, B.P. Flannery, *Numerical Recipes in C++: The Art of Scientific Computing*, Cambridge University Press, Cambridge, 2002.
[23] M.V. Sivaselvan, A.M. Reinhorn, Hysteretic models for deteriorating inelastic structures, *ASCE Journal of Engineering Mechanics* 126 (6) (2000) 633–640.